Preliminary Numerical Analysis of the LAPCAT MR2 Vehicle Configuration at Mach 8 Cruise Conditions

Pietro Roncioni, Luigi Cutrone*, Francesco Battista*, Marco Marini*, Johan Steelant***
** Centro Italiano Ricerche Aerospaziali*
Via Maiorise, 81043 Capua (CE), Italy
*** Aerothermodynamics and Propulsion Analysis Section (TEC-MPA), ESTEC-ESA*
Keplerlaan 1, P.O. Box 299, 2200 AG Noordwijk, The Netherlands

Abstract
This paper presents, in the framework of the European Union (EU) LAPCAT Program, a preliminary numerical analysis of the M8 vehicle in cruise conditions aimed at the assessment of the final configuration. Calculations for the combustion chamber analysis have been performed by means of the CIRA $C3NS_{DB}$ 3D code coupled with the integrated 1D module SPREAD. Some effects have been pointed out such as the effect of non-equilibrium recombination in the nozzle and the efficiency of the air compression process inside the inlet ramp.

1. Introduction

At present time, the most promising technology for a drastic reduction of times to destination for long-distance (i.e. from Brussels to Sydney) civil flights is the hypersonic air-breathing propulsion. At hypersonic flight speeds, turbofan engines need to be replaced above Mach 3-4 by advanced propulsion concepts like ramjet/scramjet engines. This challenge is faced in the framework of the European Union (EU) LAPCAT Program [1] that aims at providing sound technological basis for the introduction at industrial level of innovative and advanced propulsion concepts on the long-term period (20-25 years), defining the most critical RTD-building blocks to achieve this goal and finally to investigate in depth these critical technologies by developing and/or applying dedicated analytical, numerical and experimental tools. Key objectives are the definition and evaluation of different propulsion cycles and concepts, the enhancement of integrated engine/aircraft performance, mass-efficient turbines and heat exchangers, and finally high-pressure and supersonic combustion experiments and modelling. In this scenario, CIRA activities are mainly devoted to the numerical analysis of components of the vehicles or, in the case of the M8 concept, to the vehicle itself.

2. Mission profile and activity description

The activity of the present paper deals mainly with numerical simulations, at cruise flight conditions, of the LAPCAT M8 vehicle. The mission profile (Figure 1) of the M8 vehicle foresees an antipodal flight from Brussels to Sidney (> 16000 km) carrying 300 passengers with an efficient cruise at an altitude of about 30 km. The flight time is nearly 3 hours. A combination of different propulsion systems are employed for the acceleration phase of the mission, including turbojet engines based on an air-turbo rocket cycle (ATR), and dual mode ramjets [2]. For the overall performance analysis of the vehicle, the acceleration phase is of equal importance to the cruise flight, anyway this task will not be faced here. The ATR engines operate up to a Mach number of about 4.0-4.5 when the cycle is then switched to a Dual-Mode Ramjet. During previous phases of the LAPCAT program several configurations have been analyzed and a down selection is being done by a comparison of the main vehicle performances as aerodynamics, propulsion, mass estimates [1]. In this work the nose-to-tail (NtT) analysis for the MR2.4 version (Figure 2), conducted for what concerns the CIRA side, will be reported. The main aim of this work is to verify whether the aero-propulsive performances are able to sustain the vehicle (lift equal to the weight) and to maintain the velocity (thrust equal to the drag) at the cruise altitude (see Table 1). An analysis of the significant physical quantities as pressure and heat flux along the wall, average values of the main aerothermodynamic parameters along the engine axis, and the general behaviour of the vehicle will also be carried out.

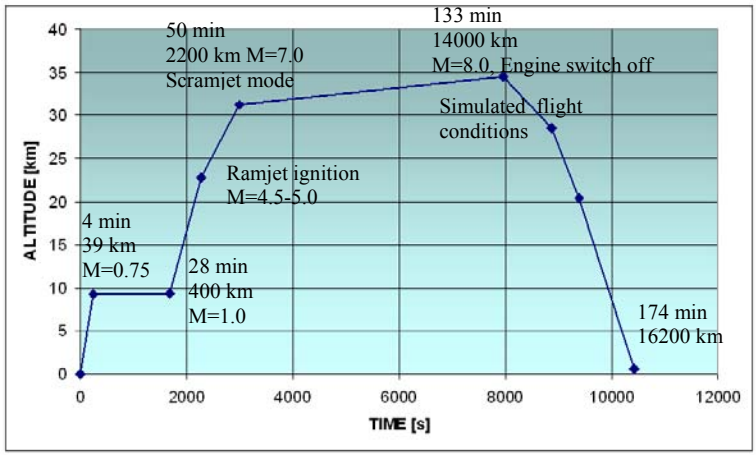

Figure 1: LAPCAT MR2.4: mission profile.

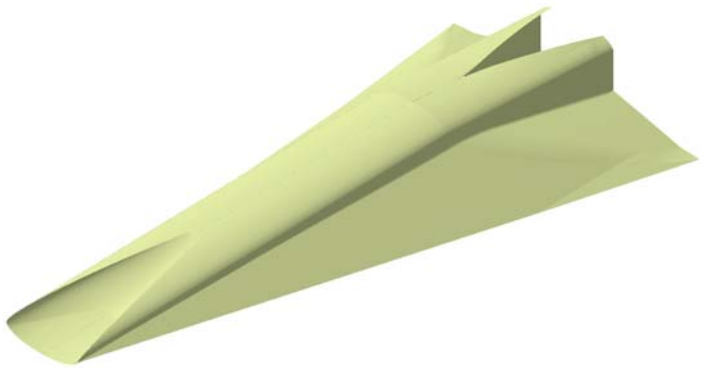

Figure 2: LAPCAT MR2.4 vehicle.

Table 1: LAPCAT M8 vehicle simulated (cruise) flight conditions.

Ma	**V**	**T**	**P**	**□**
[-]	*[m/s]*	*[K]*	*[Pa]*	*[kg/m^3]*
8.00	**2423.82**	**228.46**	**896.09**	**0.01367**

3. Numerical Methodology

3.1 C3NS$_{DB}$ CIRA Code

The numerical code used to carry out the aerothermodynamic analysis of the LAPCAT M8 vehicle is the CIRA code C3NS$_{DB}$ that solves, on a multi-block structured grid, the Reynolds Averaged Navier Stokes equations in a density-based finite volume approach with a cell centred, Flux Difference Splitting second order ENO-like upwind scheme for the convective terms [3]. The code, recently released in parallel version, has been run both on the CIRA Super Computer NEC TX-7 (scalar-parallel supercomputer with 20 1500MHz processors Itanium2, 40 GB of central memory and a total peak power of 120 GFLOPS) and on a DELL cluster of 56 cores (7 nodes with two Intel XEON 5560 2.8GHz each, with an aggregated memory of 48GB per node). Particular features of the code are, in addition to what already explained above, the multilevel approach allowing a grid sequencing and finally the multi-block/multi-inlet enabling the handling of particular initial/boundary conditions.
The physical modelling available inside the numerical code includes non-viscous (Eulerian) fluid flow and viscous laminar/transitional/turbulent flow with the work fluid being air modelled as an ideal gas or in both thermo-chemical non equilibrium and equilibrium, or a general multi-component reacting mixtures (Arrhenius formulation) [4]. A two-equation k-ε turbulence modelling is used for eddy viscosity calculation while laminar-to-turbulence transition is imposed across surface lines (i.e. a transition front). Some versions of the two-equation k-ε model are available: standard, RNG along with compressibility effects correction for high speed turbulent flows simulations [5].

3.2 SPREAD design tool

The CIRA engineering tool SPREAD (Supersonic PREliminary Aerothermodynamic Design) is conceived as a rapid design tool for a generic propulsion system (scramjet/ramjet/turbojet) [6]. It can handle a general flow physics: combustion, heat transfer, inviscid and viscous flows. Its peculiar characteristic is the high modularity being each component simulated using a black-box logic. In principle several levels of modelling can be used (0D theoretical model, Newtonian theory for panel solver, 1D/2D/3D CFD solver, etc.) at least by means of a coupling with other specific tools as CFD codes. Its main outputs are the main aero/propulsive parameters such as: drag, lift, aerodynamic efficiency, thrust, combustion efficiency, emissions and so on. A detailed chemistry modelling is available for non-equilibrium combustion simulation inside the combustion chamber. Direct and reverse design approaches are also possible.

4. Numerical Results

4.1 Grid Generation and Sensitivity Analysis

A grid has been generated for both the internal and the external part of the M8 vehicle for which the full characterization of the aerothermodynamic environment and propulsive behaviour is required. The number of blocks is 174 (63 internal and 111 external) and the number of cells is about 3.5×10^6 (0.8×10^6 internal and 2.7×10^6 external) for the finest level (L_3). Figure 3 and Figure 4 show, respectively, the block topology of the computational domain and details of the grid.

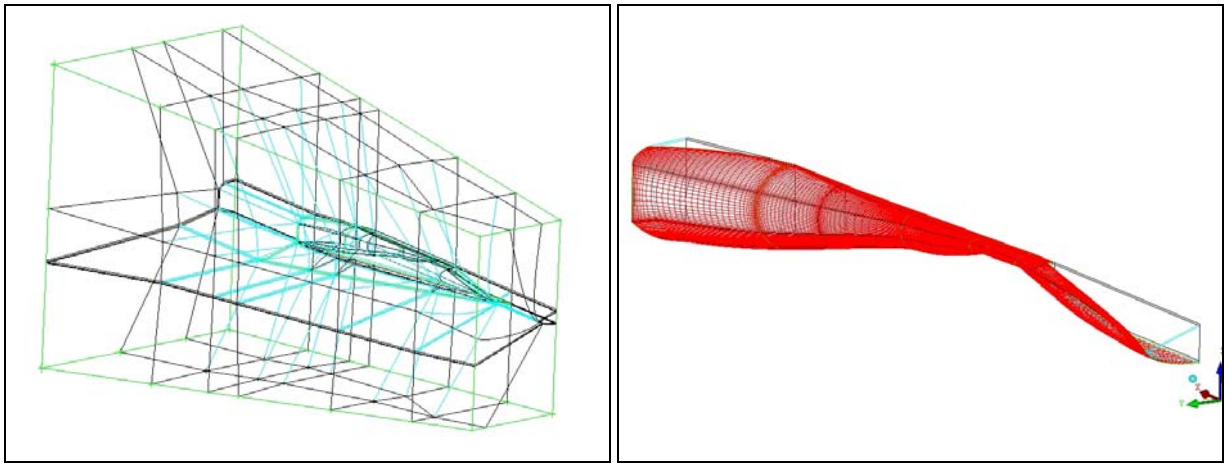

Figure 3: Block topology of full domain (left) and internal part of the vehicle (right).

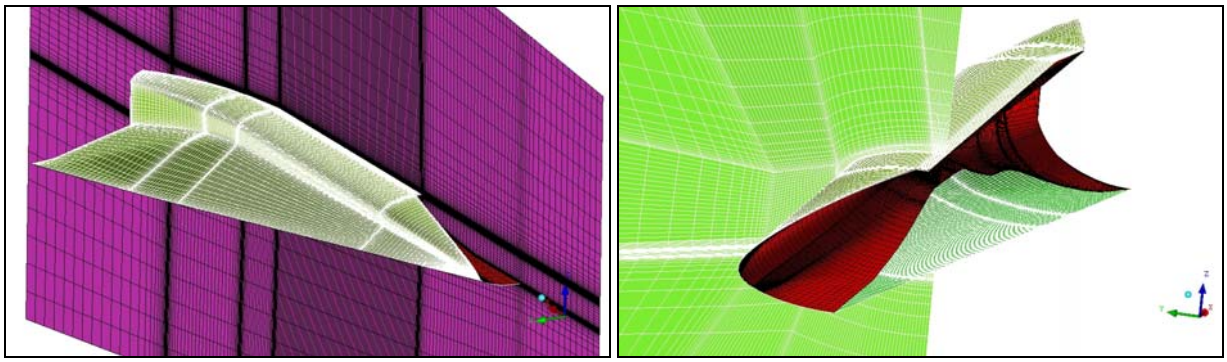

Figure 4: Body surface and symmetry plane (left), and transversal section (right).

A grid sensitivity analysis has been conducted for a fuel-on laminar case, whose results are reported, in terms of global aerodynamic forces, in Table 2 and Figure 5. The grid has been generated in such a way to have at least three levels of grid used for the sensitivity analysis. The number of cells of each level is eight times the previous level. The results show that a good grid-convergence has been reached for both lift and external drag as can be seen from Figure 5 where they are plotted in function of the number of cells.

Table 2: Grid Sensitivity: Global aerodynamic forces.

Grid level	Number of Cells	Engine state	Flow regime	L	D_{body} (ext)
[-]	*[-]*	*[-]*	*[-]*	*[tons]*	*[tons]*
L_1	54,972	*ON*	*LAM*	**336.67**	**33.11**
L_2	439,776	*ON*	*LAM*	**344.23**	**33.74**
L_3	3,518,208	*ON*	*LAM*	**348.30**	**34.94**

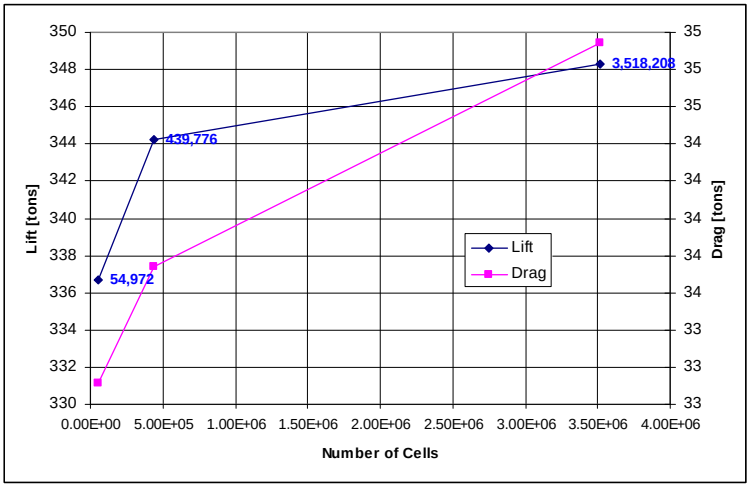

Figure 5: Grid Sensitivity: trend of Lift and Drag.

4.2 Aero/Propulsive Analysis

The numerical analysis of the LAPCAT M8 vehicle has concerned both fuel-off and fuel-on simulations at different levels of grid. The fuel-on simulations have been conducted by means of coupling with a 1D external combustion simulation tool (e.g. AbSys, Ecosim, SPREAD). In particular, a small open slot has been introduced within the constant section area combustion chamber. The two transversal surfaces of this small slot are used as outflow of the first part of the scramjet engine (intake + first part of the combustion chamber) and as inflow of the remaining part (last part of the combustion chamber + nozzle) (Figure 6). The inflow of the second part is given by the outflow of the 1D combustor simulator in terms of pressure, temperature, velocity and mixture composition. The small open slot has been removed for the fuel-off simulations for which the combustor chamber is crossed by the compressed (inside the intake) far field air. Figure 7 shows the subdivision of the scramjet engine used for the extraction the lumped aerodynamic coefficients and Figure 8-left shows the slices where the average values of the main aerothermodynamic parameters are extracted (the figure shows in particular the trend of the total pressure for a fuel-off laminar case at a L_2 grid level).

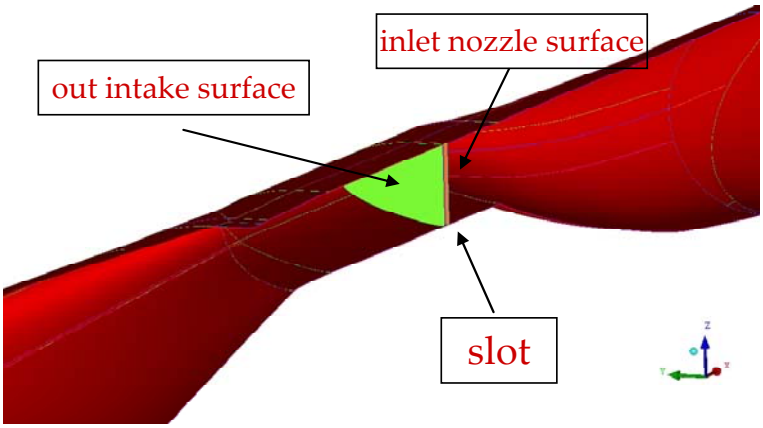

Figure 6: Small open slot within the combustor chamber.

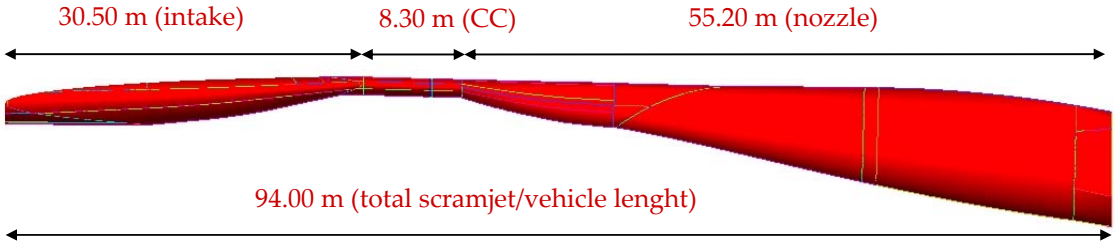

Figure 7: Internal subdivision of the vehicle.

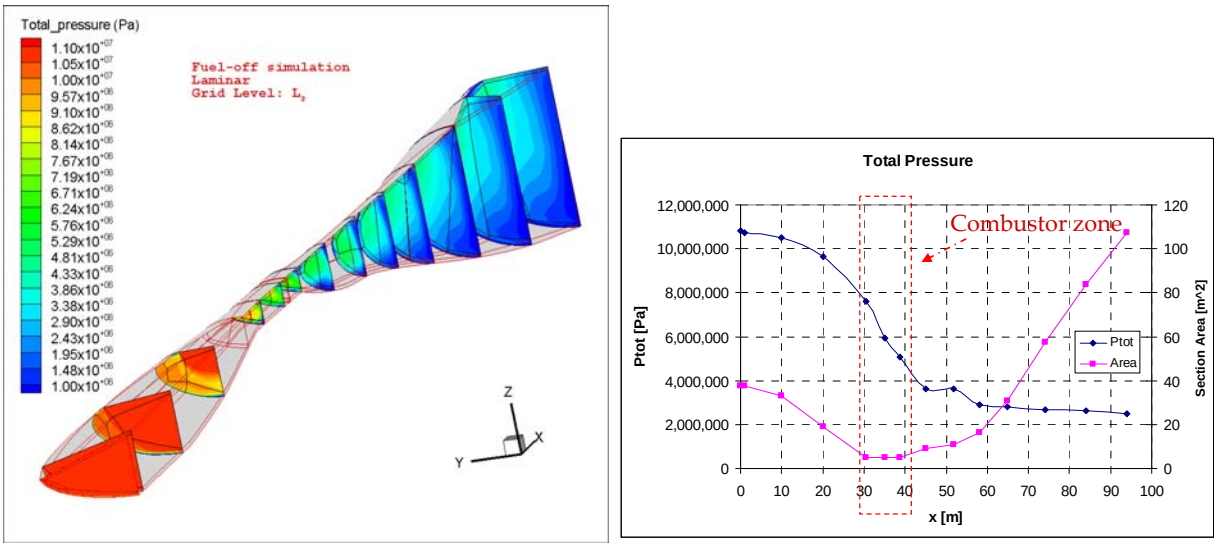

Figure 8: Total Pressure distribution along the engine. Slices on the left and average values on the right.

From Figure 8-right we can observe as the (mean) total pressure experiences a strong decrease not only along the intake but also along the combustor chamber and the first part of the nozzle. This is due to the reflection of shock waves that reaches the nozzle and continues for a quite long distance (Figure 9). The trend of the total pressure decreasing becomes regular beyond the x=60m station. The pressure recovery factor at the entrance of the combustion chamber (x=30.5 m) is about 0.7 attesting a good performance of the intake.

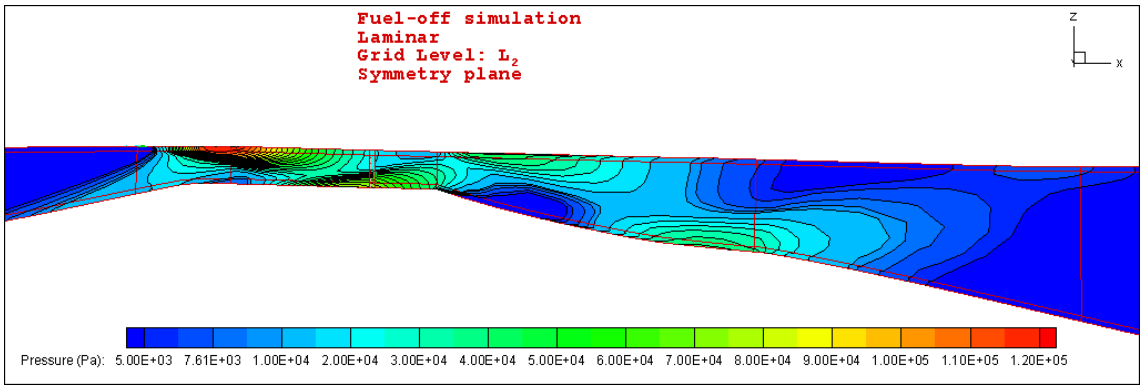

Figure 9: Static Pressure contours along the engine.

Table 3 reports, in terms of global aerodynamic coefficients, the aero/propulsive performance of the vehicle for several numerical simulations. In particular, the values of Lift and Drag are reported. This latter has been subdivided into external part (body drag) and internal part (engine drag, namely the net thrust). The fuel-on simulations have been performed starting from post-combustion conditions given by ESTEC (products of combustion of air and H_2 at an Equivalence Ratio ER=0.6). The following main conclusions can be highlighted for the values of the table: for all simulations the value of Lift is greater than 340 tons, the aero-propulsive balance is positive ($D_{prop} < 0$) for both

laminar and turbulent simulations in fuel-on conditions, The net thrust (Intake + Combustion Chamber + Nozzle) is able to compensate the external Drag (there is a residual thrust of 16.29 tons for the turbulent fuel-on case), thus ensuring a constant altitude hypersonic cruise.

Table 3: Aero/propulsive performance.

Grid level	Engine state	Flow regime	L	D_{tot} (ext + int)	D_{body} (ext)	D_{prop} (int)	D_{intake}	D_{cc}	D_{nozzle}
[-]	*[-]*	*[-]*	*[tons]*	*[tons]*	*[tons]*	*[tons]*	*[tons]*	*[tons]*	*[tons]*
L_1	*OFF*	*LAM*	**342.99**	**46.06**	**33.14**	**12.92**	18.02	0.59	-5.69
L_2	*OFF*	*LAM*	**351.77**	**46.47**	**33.27**	**13.20**	17.97	0.57	-5.34
L_3	*OFF*	*LAM*	**360.16**	**47.19**	**33.56**	**13.64**	17.98	0.62	-4.96
L_3	*ON*	*LAM*	**348.30**	**-24.68**	**34.94**	**-59.62**	18.03	1.52	-79.17
L_3	*ON*	*TURB*	**342.37**	**-16.29**	**37.61**	**-53.90**	20.61	3.37	-77.89

Figure 10 shows the values of average Mach number along the scramjet engine for several numerical simulations both in fuel-on and fuel-off conditions. We can see the discontinuity of Mach number where the combustion process instantaneously takes place thanks to the 1D external tool coupling.

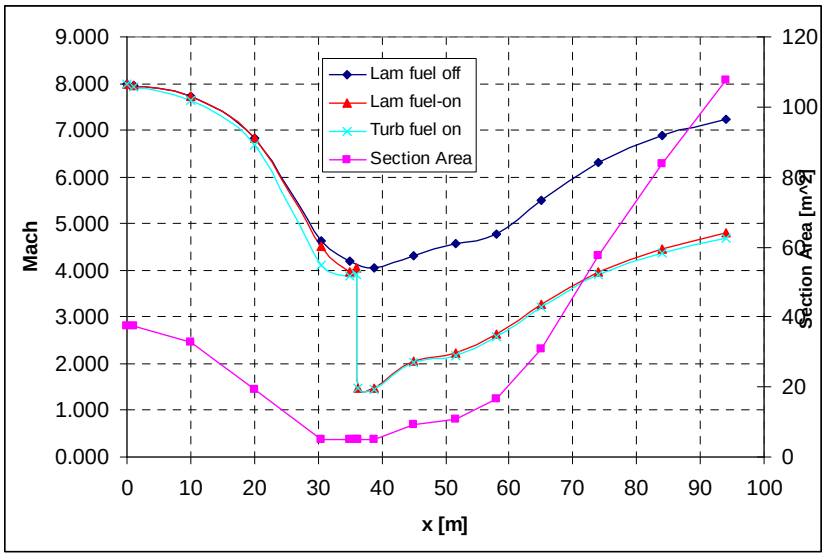

Figure 10: Mach number contours along the engine for several simulations.

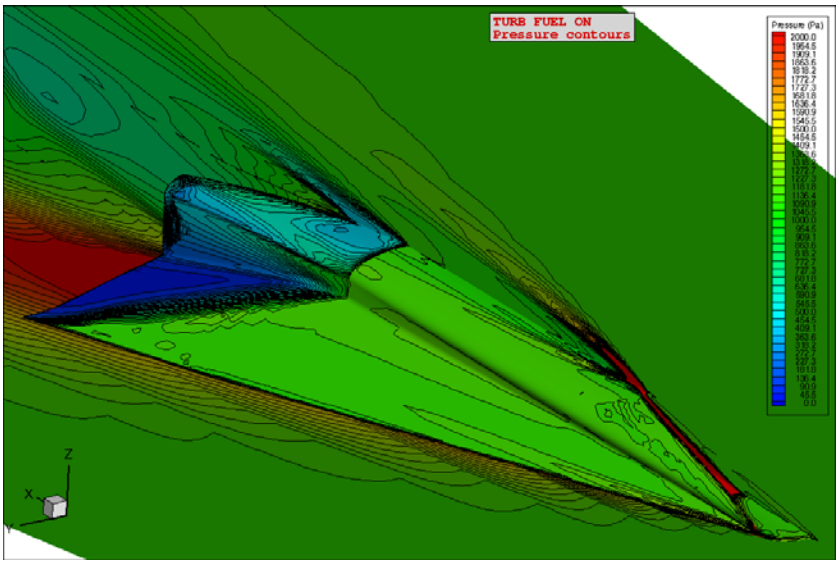

Figure 11: Pressure contours over the body.

The predicted pressure distributions over the body (Figure 11) shows the strong expansion region on the leeside and the interaction between leeside flow and exit nozzle flow, thus forming the vehicle's wake.

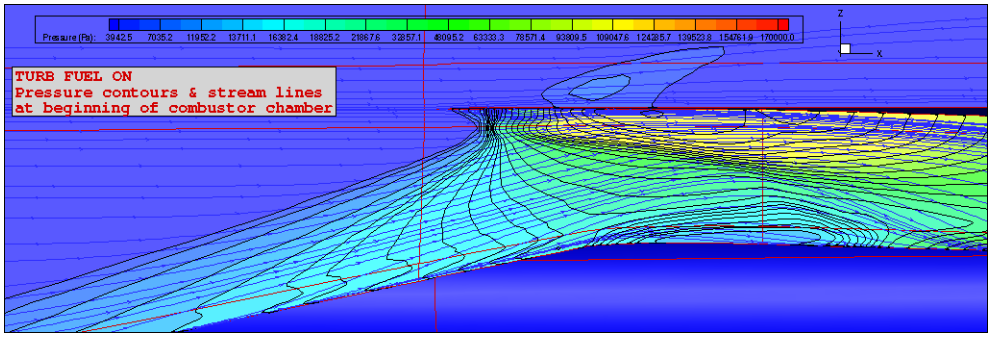

Figure 12: Pressure contours on the symmetry plane.

The pressure distributions on the symmetry plane near the intake crotch highlights the following phenomena: a strong shock-wave boundary-layer interaction near the cowl where the coalescence of compression waves occurs; a local separation zone and a smeared reflection of the oblique shock waves impinging at this point; near the crotch, a boundary layer develops at this point resulting in a lambda-interaction.
The skin friction lines distribution over the internal walls (Figure 13) can give us an idea of the general flow behaviour inside the engine, and in particular: a local separation at the crotch and incipient separation conditions on the internal surface; a highly three-dimensional flow at the combustor entrance; a separation line on the lateral surface of the combustor, the presence of vortical structures.

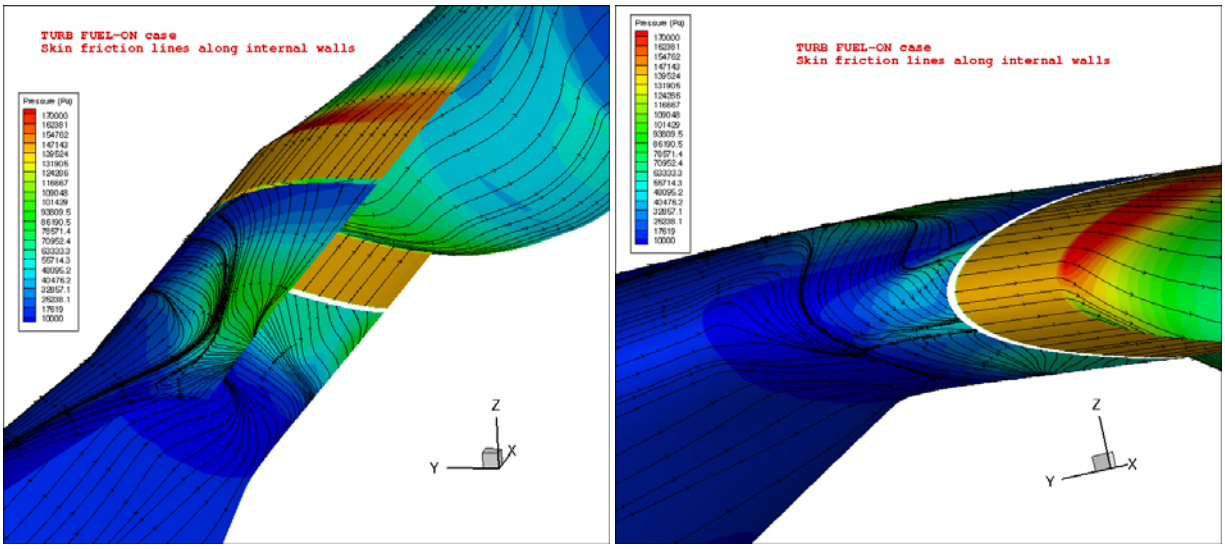

Figure 13: Skin friction lines distribution over the internal walls (scramjet engine).

5. Conclusions

Preliminary numerical simulations of the LAPCAT M8 MR2.4 hypersonic vehicle have been performed both in fuel-off and fuel-on conditions. The fuel-on simulations have been performed starting from post-combustion conditions provided by an external 1D combustor simulator (and so in the hypothesis that the combustion occurs along the combustor chamber).
The global results have shown values of Lift greater than 340 tons and values of net Thrust greater than the Drag, thus ensuring the high altitude hypersonic cruise. A deeper analysis of results has shown a shock-wave boundary-layer interaction near the cowl (i.e. at the crotch) that causes a local separation and a not optimized system of shock reflections at the combustor entrance, with highly three-dimensional flow and possible presence of separation and vortex structures.

Acknowledgements

This work was performed within the 'Long-Term Advanced Propulsion Concepts and Technologies II' project investigating high-speed transport. LAPCAT II, coordinated by ESA-ESTEC, is supported by the EU within the 7th Framework Programme Theme7 Transport, Contract no.: ACP7-GA-2008-211485. Further info on LAPCAT II can be found on http://www..esa.int/techresources/lapcat_II.

References

[1] J. Steelant. 2011. Sustained Hypersonic Flight in Europe: First Technology Achievements within LAPCAT II. *17th AIAA International Space Planes and Hypersonic Systems and Technologies Conference, 11 - 14 April 2011, San Francisco, California. AIAA-2011-2243.*

[2] Murray N., Steelant J and Mack A. 2010. Design Evolution for Highly Integrated Hypersonic Vehicles. *Space Propulsion 2010, San Sebastian, Spain, 3-6 May 2010.*

[3] Battista F., Cutrone L., Ranuzzi G. 2008. C3NS Solver for Supersonic Combustion Simulations. *CIRA LAPCAT Report CIRA-CF-08-0484*.

[4] Jachimowski C.J. 1998. An Analytical Study of Hydrogen-Air Reaction Mechanism with Application to Scramjet Combustion. *NASA-TP-2791.*

[5] Grasso F., Falconi D. 2001. Shock-Wave/Turbulent Boundary-Layer Interactions in Nonequilibrium Flows. *AIAA Journal, Vol. 39, No. 11, 2131-2140, November 2001*.

[6] Bonelli F., Cutrone L., Votta R., Viggiano A., Magi V. 2011. Preliminary design of a hypersonic air-breathing vehicle. *17th AIAA/AHI Space Planes and Hypersonic Systems and Technologies Conference, San Francisco, US, AIAA-2011-2319.*